Steel and Composite Structures, *Vol. 32, No. 6 (2019) 795-806*
DOI: https://doi.org/10.12989/scs.2019.32.6.795

Vibration analysis of sandwich beam with nanocomposite facesheets considering structural damping effects

Ali Cheraghbak, M. Botshekanan Dehkordi* and H. Golestanian

Faculty of Engineering, Shahrekourd University, Shahrekord, Iran

(*Received May 5, 2019, Revised July 31, 2019, Accepted August 27, 2019*)

Abstract. In this paper, free vibration of sandwich beam with flexible core resting on orthotropic Pasternak is investigated. The top and bottom layers are reinforced by carbon nanotubes (CNTs). This sandwich structural is modeled by Euler and Frostig theories. The effect of agglomeration using Mori-Tanaka model is considered. The Eringen's theory is applied for size effect. The structural damping is investigated by Kelvin-voigt model. The motion equations are calculated by Hamilton's principle and energy method. Using analytical method, the frequency of the structure is obtained. The effect of agglomeration and CNTs volume percent for different parameter such as damping of structure, thickens and spring constant of elastic medium are presented on the frequency of the composite structure. Results show that with increasing CNTs agglomeration, frequency is decreased.

Keywords: free vibration; sandwich beam; CNTs; agglomeration; orthotropic pasternak medium

1. Introduction

Among nano composites, the polymeric nano composites have been intense interest among researchers. One of the reasons for the development of polymeric nano composites is unique mechanical, chemical and physical properties. Polymeric nano composites usually have high strength, low weight, high thermal stability, high electrical conductivity and high chemical resistance. By adding a few percent of the nanoparticles to a pure polymer, Tensile strength, yield strength and yang modulus increase significantly. For example, by adding only 0.04% of the volume of Mica (a type of silicate) with a dimension of 50 nm to Epoxy, the modulus Yang will increase the 58%

Buckling behavior of sandwich panels with a core that is flexible in the out-of-plane direction, also denoted as "soft" core including high-order effects, was presented by Frostig (2003). Propagation of flexural and shear waves in an unbounded sandwich beam were considered by Sorokin and Grishina (2004). An elementary theory for non-linear vibrations of viscoelastic sandwich beams was presented by Daya *et al*. (2004). An efficient new coupled zigzag theory was developed by Kapuria *et al*. (2005) for dynamics of piezoelectric composite and sandwich beams with damping. The dynamic response of a fully clamped metallic sandwich beam subjected to impulsive loading was theoretically investigated by Qin and Wang (2009). Liu *et al*. (2012) presented a new Fourier-related double scale analysis to study instability phenomena of sandwich structures. Using the membrane factor method, we obtained the analytical solutions for the dynamic response of the sandwich beam. An analytical model for face wrinkling failure under dynamic compression of corrugated core sandwich columns was investigated by Lim and Bart-Smith (2015). Sandwich panels were produced by Lakreb *et al*. (2015) using wood veneer of Aleppo pine as face sheets and cork agglomerate as core, including multilayered designs, for use in construction. A new refined hyperbolic shear and normal deformation beam theory was developed by Bennai *et al*. (2015) to study the free vibration and buckling of functionally graded (FG) sandwich beams under various boundary conditions. Vibration analysis of embedded functionally graded (FG)-carbon nanotubes (CNT)-reinforced piezoelectric cylindrical shell subjected to uniform and non-uniform temperature distributions were presented by Madani *et al*. (2016). Eltaher *et al*. (2016) investigated the effects of both size-dependency and material-dependency on the nonlinear static behavior of carbon nanotubes (CNTs). The nonlinear eigen frequency response of the functionally graded single-walled carbon nanotube reinforced sandwich structure was investigated by Mehar *et al*. (2017) numerically considering the Green-Lagrange nonlinear strain under uniform thermal environment. Smyczynski and Magnucka-Blandzi (2018) devoted to the stability analysis of a simply supported five layer sandwich beam. Agglomeration phenomenon of CNTs was experimentally observed and then it was analytically modeled by Zeinedini *et al*. (2018). Using a base wash procedure, oxygen functional groups have been removed the graphene oxide (GO) flakes, and the prepare the base-washed GO (BwGO) flakes obtained have been Incorporated into a PVA matrix to make a nano composite was studied by Li *et al*. (2018). Shokravi (2018) presented forced vibration of micro cylindrical shell reinforced by functionally graded carbon nanotubes (FGCNTs). Safaei *et al*. (2018) investigated the effect of thermal gradient load on natural frequencies of sandwich plates with polymer-based

*Corresponding author, Ph.D., Associate Professor,
E-mail: mbd_dehkordi@yahoo.com

http://www.techno-press.org/?journal=scs&subpage=6
ISSN: 1229-9367 (Print), 1598-6233 (Online)

nanocomposite face sheets reinforced by functionally graded (FG) single-walled carbon nano tubes (SWCNTs) agglomerations. Critical comparison of different mean field homogenization approaches for CNT-reinforced polymer composites with waviness and agglomeration effects was presented by García-Macías and Castro-Triguero (2018).

The study of composite and nanocomposite paltes was presented by Duc *et al*. (Duc and Minh 2010, Duc 2014a, b, 2016, Duc *et al*. 2013, 2015, 2018). Chung *et al*. (2013) investigated Polymeric Composite Films Using Modified TiO2 Nanoparticles. Large amplitude vibration problem of laminated composite spherical shell panel under combined temperature and moisture environment was analyzed by Mahapatra and Panda (2016). The nonlinear free vibration behaviour of laminated composite spherical shell panel under the elevated hygrothermal environment was investigated by Mahapatra *et al*. (2016a). Mahapatra *et al*. (2016b) studied the geometrically nonlinear transverse bending behavior of the shear deformable laminated composite spherical shell panel under hygro-thermo-mechanical loading. Nonlinear free vibration behavior of laminated composite curved panel under hygrothermal environment was investigated by Mahapatra *et al*. (2016c). The flexural behaviour of the laminated composite plate embedded with two different smart materials (piezoelectric and magnetostrictive) and subsequent deflection suppression were investigated by Dutta *et al*. (2017). Suman *et al*. (2017) studied static bending and strength behaviour of the laminated composite plate embedded with magnetostrictive (MS) material numerically using commercial finite element tool. Vibration and nonlinear dynamic response of eccentrically stiffened functionally graded composite truncated conical shells in thermal environments were presented by Chan *et al*. (2018). Nonlinear response and buckling analysis of eccentrically stiffened FGM toroidal shell segments in thermal environment were studied by Vuong and Duc (2018). In this work, buckling analyses of composite concrete plate reinforced by Piezoelectric nanoparticles is studied.

In this paper, vibration of sandwich beams with flexible core and nanocomposite facesheets is presented. The top and bottom layers are reinforced with CNTs considering the agglomeration effects. The sandwich structure is modeled by Frostig theory for core and Euler-Bernoulli model for facesheets. Applying Hamilton's principle, the motion equations are derived and based on Navier method, the frequency of the structure is calculated. The effect of agglomeration and CNTs volume percent for different parameter such as damping of structure, thickens and spring constant of elastic medium are presented on the frequency of the composite structure.

2. Kinematics of different theories

Fig. 1 shows a sandwich beam including top and bottom beams reinforced with CNTs and flexible core resting on elastic medium with length of L, core thickness of c and top and bottom layers thickness d_t and d_b, respectively.

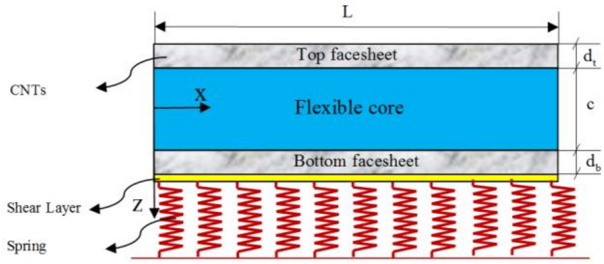

Fig. 1 A schematic of sandwich beam with nanocomposite facesheets resting on elastic medium

2.1 Strain-stress relations

The strain-stress relations for the facesheets can be given as follows

$$\sigma_{xx}^{t} = E^{t}\varepsilon_{xx}^{t}, \tag{1}$$

$$\sigma_{xx}^{b} = E^{b}\varepsilon_{xx}^{b}, \tag{2}$$

where, parameters $E^t$and $E^b$are Young modulus of upper and lower beam, respectively. The strain-stress relations for core can be given

$$T = G_c\gamma, \tag{3}$$

$$\sigma_{zz} = E_c\frac{\partial}{\partial z}w_c, \tag{4}$$

where, parameters $G_c$and $E_c$are shear modulus and Young modulus of the core, respectively. Based on the refined first order Forstig theory, the strains can be written as

$$\gamma_c = \frac{\partial}{\partial z}u_c - z\frac{\partial}{\partial x}w_c, \tag{5}$$

$$\varepsilon_{zz} = \frac{\partial}{\partial z}w_c, \tag{6}$$

The kinematic unknown parameters of the refined first order Forstig theory are $u_c$and w_c which are the axial and transverse core displacements, respectively.

2.2 Euler–Bernoulli model

Based on Euler–Bernoulli beam model, the orthogonal components of the displacement vector can be written as

$$u(x,z,t) = u_0(x,t) - z\frac{\partial w_0(x,t)}{\partial x}, \tag{7}$$

$$w(x,z,t) = w_0(x,t), \tag{8}$$

The strain–displacement relations for the facesheets can be express as

$$\varepsilon_{xx}^{t} = \frac{\partial}{\partial x}u_{ot} - z\frac{\partial^2}{\partial x^2}w_b, \tag{9}$$

$$\varepsilon_{xx}^{b} = \frac{\partial}{\partial x}u_{ob} - z\frac{\partial^2}{\partial x^2}w_b, \tag{10}$$

where the superscripts (t, b) are used to denote quantities corresponding to the upper and lower beam, respectively.

2.3 Variation of potential energy

The variation of potential energy for beams and flexible core can be written as

$$\delta U = \int_{u_{top}} \sigma_{xx}\delta\varepsilon_{xx}du + \int_{u_{bot}} \sigma_{xx}\delta\varepsilon_{xx}du + \int_{u_{core}} \tau_c\delta\gamma_c du + \int_{u_{core}} \sigma_{zz}\delta\varepsilon_{zz}du \tag{11}$$

where, the force and moment resultants can be defined as

$$N_{txx} = \int_{A^t} \sigma_{xx}^{t}\, dA = -E^t A_t \frac{\partial}{\partial x}u_{ot}, \tag{12}$$

$$N_{bxx} = \int_{A^b} \sigma_{xx}^{b}\, dA = -E^b A_b \frac{\partial}{\partial x}u_{ob}, \tag{13}$$

$$M_{txx} = \int_{A^t} \sigma_{xx}^{t} z\, dA = -E^t I_t \frac{\partial^2}{\partial x^2}w_t, \tag{14}$$

$$M_{bxx} = \int_{A^b} \sigma_{xx}^{t} z dA = -E^b I_b \frac{\partial^2}{\partial x^2}w_b, \tag{15}$$

2.4 Variation of kinematic energy

The variation of kinematic can be given as follows

$$\delta K = \int_{t_1}^{t_2}\left[\begin{gathered}\int_0^L m_t(\dot{u}_{ot}\delta\dot{u}_{ot} + \dot{w}_t\delta\dot{w}_t)\,dx \\ + \int_0^L m_b(\dot{u}_{ob}\delta\dot{u}_{ob} + \dot{w}_b\delta\dot{w}_b)\,dx \\ + \int_{v_{core}} \rho_c\dot{u}_c\delta\dot{u}_c dv + \int_{v_{core}} \rho_c\dot{w}_c\delta\dot{w}_c dv\end{gathered}\right]dt \tag{16}$$

2.5 Variation of external work

The variation of external work, due to elastic medium load simulated by orthotropic Pasternak model can be express as (Kutlu *et al*. 2012)

$$\delta W = \int \left(\begin{gathered} kg_1 \cos^2(\theta)\frac{\partial^2}{\partial x^2}w_b + \\ kg_2 \sin^2(\theta)\frac{\partial^2}{\partial x^2}w_b - k_w w_b\end{gathered}\right)dx \tag{17}$$

2.6 Motion equation

For driving the motion equation, the Hamilton principle is used as follows

$$\int (\delta U - \delta W - \delta K)dt = 0 \tag{18}$$

where δ is variation, $\delta U$is variation of potential energy, δW is variation of kinematic energy and δK is variation of external work.

Using the Hamilton principle and partial integral, the governing equations are computed

Equation 1:

$$\begin{gathered}\frac{\partial N_{txx}}{\partial x} + \tau_b - m_t\frac{\partial^2}{\partial t^2}u_{ot} - \frac{m_c}{3}\frac{\partial^2}{\partial t^2}u_{ot} \\ -\frac{m_c}{6}\frac{\partial^2}{\partial t^2}u_{ob} + \frac{m_c d_t}{6}\frac{\partial^3}{\partial t^2\partial x}w_t \\ +\frac{m_c d_b}{12}\frac{\partial^3}{\partial t^2\partial x}w_b + m_{1t}\frac{\partial^3}{\partial t^2\partial x}w_t = 0,\end{gathered} \tag{19}$$

Equation 2:

$$\begin{gathered}\frac{\partial N_{bxx}}{\partial x} - \tau_b - m_b\frac{\partial^2}{\partial t^2}u_{ot} - \frac{m_c}{6}\frac{\partial^2}{\partial t^2}u_{ot} \\ -\frac{m_c}{3}\frac{\partial^2}{\partial t^2}u_{ob} + \frac{m_c d_t}{12}\frac{\partial^3}{\partial t^2\partial x}w_t \\ -\frac{m_c d_b}{6}\frac{\partial^3}{\partial t^2\partial x}w_b + m_{1b}\frac{\partial^3}{\partial t^2\partial x}w_b = 0,\end{gathered} \tag{20}$$

Equation 3:

$$\begin{gathered}\frac{\partial^2 M_{txx}}{\partial x^2} + \frac{bd_t}{2}\frac{\partial\tau}{\partial x} + \left(\frac{E_c.(w_b - w_t)}{c} + \frac{c}{2}\frac{\partial\tau}{\partial x}\right)b \\ -m_t\frac{\partial^2}{\partial t^2}w_t - \frac{m_c d_t}{6}\frac{\partial^3}{\partial t^2\partial x}u_{ot} - \frac{m_c d_b}{12}\frac{\partial^3}{\partial t^2\partial x}u_{ob} \\ +\frac{m_c d_t^2}{12}\frac{\partial^3}{\partial t^2\partial x}w_t - \frac{m_c d_b d_t}{24}\frac{\partial^3}{\partial t^2\partial x}w_b \\ - m_{1t}\frac{\partial^3}{\partial t^2\partial x}u_{ot} \\ +m_{2t}\frac{\partial^4}{\partial t^2\partial x^2}w_t - \frac{m_c}{6}\frac{\partial^2}{\partial t^2}w_b - \frac{m_c}{3}\frac{\partial^2}{\partial t^2}w_t = 0,\end{gathered} \tag{21}$$

Equation 4:

$$\begin{gathered}\frac{\partial^2 M_{bxx}}{\partial x^2} + \frac{bd_b}{2}\frac{\partial\tau}{\partial x} - \left(\frac{E_c(w_b - w_t)}{c} - \frac{c}{2}\frac{\partial\tau}{\partial x}\right)b \\ -m_b\frac{\partial^2}{\partial t^2}w_b + \frac{m_c d_b}{12}\frac{\partial^3}{\partial t^2\partial x}u_{ot} + \frac{m_c d_b}{6}\frac{\partial^3}{\partial t^2\partial x}u_{ob} \\ +\frac{m_c d_b^2}{12}\frac{\partial^3}{\partial t^2\partial x}w_b - \frac{m_c d_b d_t}{24}\frac{\partial^3}{\partial t^2\partial x}w_t \\ -m_{1b}\frac{\partial^3}{\partial t^2\partial x}u_{ob} + m_{2b}\frac{\partial^4}{\partial t^2\partial x^2}w_b - \frac{m_c}{6}\frac{\partial^2}{\partial t^2}w_t \\ -\frac{m_c}{3}\frac{\partial^2}{\partial t^2}w_b - kg_1\cos^2(\theta)\frac{\partial^2}{\partial x^2}w_b \\ +kg_2\sin^2(\theta)\frac{\partial^2}{\partial x^2}w_b - k_w w_b = 0,\end{gathered} \tag{22}$$

Equation 5:

$$\begin{gathered}u_{0t}b - u_{0b}b - \frac{b(c - d_t)}{2}\frac{\partial w_t}{\partial x} - \frac{b(c - d_b)}{2}\frac{\partial w_b}{\partial x} \\ -\frac{bc^3}{12E_c}\frac{\partial^2\tau}{\partial x^2} - \frac{\tau_b c}{G_c} = 0,\end{gathered} \tag{23}$$

2.7 Viscoelastic theory

Viscoelastic is composed of visco and elastic parameters. The material properties of system are assumed viscoelastic using Kelvin–Voigt model. So the elastic parameters of core and facesheets can be given as (Kolahchi 2017)

$$E^t = E^t \left(1 + g\frac{\partial}{\partial t}\right), \tag{24}$$

$$E^b = E^b \left(1 + g\frac{\partial}{\partial t}\right), \tag{25}$$

$$E_c = E_c \left(1 + g\frac{\partial}{\partial t}\right), \tag{26}$$

2.8 Mori-Tanaka Model and agglomeration effects

In this section, the effective modulus of the composite shell reinforced by CNTs is developed. Different methods are available to estimate the overall properties of a composite. Due to its simplicity and accuracy even at high volume fractions of the inclusions, the Mori-Tanaka method is employed in this section. To begin with, the CNTs are assumed to be aligned and straight with the dispersion of uniform in the polymer. The matrix is assumed to be elastic and isotropic, with the Young's modulus E_m and the Poisson's ratioυ_m. The constitutive relations for a layer of the composite with the principal axes parallel to the r, θ and z directions are (Mori and Tanaka 1973)

$$\begin{Bmatrix}\sigma_{11}\\ \sigma_{22}\\ \sigma_{33}\\ \sigma_{23}\\ \sigma_{13}\\ \sigma_{12}\end{Bmatrix} = \begin{bmatrix} k+m & l & k-m & 0 & 0 & 0\\ l & n & l & 0 & 0 & 0\\ k-m & l & k+m & 0 & 0 & 0\\ 0 & 0 & 0 & p & 0 & 0\\ 0 & 0 & 0 & 0 & m & 0\\ 0 & 0 & 0 & 0 & 0 & p\end{bmatrix} \begin{Bmatrix}\varepsilon_{11}\\ \varepsilon_{22}\\ \varepsilon_{33}\\ \gamma_{23}\\ \gamma_{13}\\ \gamma_{12}\end{Bmatrix} \tag{27}$$

Where σ_{ij}, ε_{ij}, γ_{ij}, k, m, n, l, p are the stress components, the strain components and the stiffness coefficients respectively. According to the Mori-Tanaka method the stiffness coefficients are given by

$$k = \frac{E_m\{E_m c_m + 2k_r(1+\nu_m)[1 + c_r(1-2\nu_m)]\}}{2(1+\nu_m)[E_m(1 + c_r - 2\nu_m) + 2c_m k_r(1 - \nu_m - 2\nu_m^2)]}$$

$$l = \frac{E_m\{c_m\nu_m[E_m + 2k_r(1+\nu_m)] + 2c_r l_r(1-\nu_m^2)]\}}{(1+\nu_m)[E_m(1 + c_r - 2\nu_m) + 2c_m k_r(1 - \nu_m - 2\nu_m^2)]} \tag{28}$$

$$n = \frac{E_m^2 c_m(1 + c_r - c_m\nu_m) + 2c_m c_r(k_r n_r - l_r^2)(1+\nu_m)^2(1-2\nu_m)}{(1+\nu_m)[E_m(1 + c_r - 2\nu_m) + 2c_m k_r(1 - \nu_m - 2\nu_m^2)]} + \frac{E_m[2c_m^2 k_r(1-\nu_m) + c_r n_r(1 + c_r - 2\nu_m) - 4c_m l_r \nu_m]}{E_m(1 + c_r - 2\nu_m) + 2c_m k_r(1 - \nu_m - 2\nu_m^2)}$$

$$p = \frac{E_m[E_m c_m + 2p_r(1+\nu_m)(1+c_r)]}{2(1+\nu_m)[E_m(1+c_r) + 2c_m p_r(1+\nu_m)]} \tag{28}$$

$$m = \frac{E_m[E_m c_m + 2m_r(1+\nu_m)(3 + c_r - 4\nu_m)]}{2(1+\nu_m)\{E_m[c_m + 4c_r(1-\nu_m)] + 2c_m m_r(3 - \nu_m - 4\nu_m^2)\}}$$

Where C_m and C_r are the volume fractions of the matrix and the CNTs respectively *and kr*, l_r, n_r, p_r, m_r are the Hills elastic modulus for the CNTs (Loghman and Cheraghbak 2016). The experimental results show that the most of CNTs are bent and centralized in one area of the polymer. These regions with concentrated CNTs are assumed in this section to have spherical shapes, and are considered as ''inclusions'' with different elastic properties from the surrounding material. The total volume V_r of CNTs can be divided into the following two parts

$$V_r = V_r^{inclusion} + V_r^m \tag{29}$$

Where $V_r^{inclusion}$ and V_r^m are the volumes of CNTs dispersed in the inclusions ~concentrated regions! and in the matrix, respectively. Introduce two parameters ξ and ζ describe the agglomeration of CNTs

$$\xi = \frac{V_{inclusion}}{V}, \tag{30}$$

$$\zeta = \frac{V_r^{inclusion}}{V_r}. \tag{31}$$

However, the average volume fraction c_r of CNTs in the composite is

$$C_r = \frac{V_r}{V}. \tag{33}$$

Assume that all the orientations of the CNTs are completely random. Hence, the effective bulk modulus (*K*) and effective shear modulus (*G*) may be written as

$$K = K_{out}\left[1 + \frac{\xi\left(\frac{K_{in}}{K_{out}} - 1\right)}{1 + \alpha(1-\xi)\left(\frac{K_{in}}{K_{out}} - 1\right)}\right], \tag{33}$$

$$G = G_{out}\left[1 + \frac{\xi\left(\frac{G_{in}}{G_{out}} - 1\right)}{1 + \beta(1-\xi)\left(\frac{G_{in}}{G_{out}} - 1\right)}\right], \tag{34}$$

Where

$$K_{in} = K_m + \frac{(\delta_r - 3K_m\chi_r)C_r\zeta}{3(\xi - C_r\zeta + C_r\zeta\chi_r)}, \tag{35}$$

$$K_{out} = K_m + \frac{C_r(\delta_r - 3K_m\chi_r)(1-\zeta)}{3[1 - \xi - C_r(1-\zeta) + C_r\chi_r(1-\zeta)]}, \tag{36}$$

$$G_{in} = G_m + \frac{(\eta_r - 3G_m\beta_r)C_r\zeta}{2(\xi - C_r\zeta + C_r\zeta\beta_r)}, \tag{37}$$

$$G_{out} = G_m + \frac{C_r(\eta_r - 3G_m\beta_r)(1-\zeta)}{2[1 - \xi - C_r(1-\zeta) + C_r\beta_r(1-\zeta)]}, \tag{38}$$

Where $\chi_r, \beta_r, \delta_r, \eta_r$ may be calculated as

$$\chi_r = \frac{3(K_m + G_m) + k_r - l_r}{3(k_r + G_m)}, \tag{39}$$

$$\beta_r = \frac{1}{5}\begin{Bmatrix} \dfrac{4G_m + 2k_r + l_r}{3(k_r + G_m)} + \dfrac{4G_m}{(p_r + G_m)} \\ + \dfrac{2[G_m(3K_m + G_m) + G_m(3K_m + 7G_m)]}{G_m(3K_m + G_m) + m_r(3K_m + 7G_m)} \end{Bmatrix}, \quad (40)$$

$$\delta_r = \frac{1}{3}\left[n_r + 2l_r + \frac{(2k_r - l_r)(3K_m + 2G_m - l_r)}{k_r + G_m}\right], \quad (41)$$

$$\eta_r = \frac{1}{5}\begin{bmatrix} \dfrac{2}{3}(n_r - l_r) + \dfrac{4G_m p_r}{(p_r + G_m)} + \\ \dfrac{8G_m m_r(3K_m + 4G_m)}{3K_m(m_r + G_m) + G_m(7m_r + G_m)} \\ + \dfrac{2(k_r - l_r)(2G_m + l_r)}{3(k_r + G_m)} \end{bmatrix}. \quad (42)$$

Where, K_m and G_m are the bulk and shear moduli of the matrix which can be written as

$$K_m = \frac{E_m}{3(1 - 2\upsilon_m)}, \quad (43)$$

$$G_m = \frac{E_m}{2(1 + \upsilon_m)}. \quad (44)$$

Furthermore, β, α can be obtained from

$$\alpha = \frac{(1 + \upsilon_{out})}{3(1 - \upsilon_{out})}, \quad (45)$$

$$\beta = \frac{2(4 - 5\upsilon_{out})}{15(1 - \upsilon_{out})}, \quad (46)$$

$$\upsilon_{out} = \frac{3K_{out} - 2G_{out}}{6K_{out} + 2G_{out}}. \quad (47)$$

Finally, the elastic modulus (E) and poison's ratio (υ) can be calculated as

$$E = \frac{9KG}{3K + G}, \quad (48)$$

$$\upsilon = \frac{3K - 2G}{6K + 2G}. \quad (49)$$

Therefore, the governing equations of sandwich beam can be written as

$$\begin{aligned} &-E^t A_t\left[\frac{\partial^2}{\partial x^2}u_{ot} + g.\frac{\partial^3}{\partial x^2 \partial t}u_{ot}\right] + \tau_b \\ &-m_t\frac{\partial^2}{\partial t^2}u_{ot} - \frac{m_c}{3}\frac{\partial^2}{\partial t^2}u_{ot} - \frac{m_c}{6}\frac{\partial^2}{\partial t^2}u_{ob} \\ &+\frac{m_c d_t}{6}\frac{\partial^3}{\partial t^2 \partial x}w_t + \frac{m_c d_b}{12}\frac{\partial^3}{\partial t^2 \partial x}w_b \\ &+m_{1t}\frac{\partial^3}{\partial t^2 \partial x}w_t = 0, \end{aligned} \quad (50)$$

$$\begin{aligned} &-E^b A_b\left[\frac{\partial^2}{\partial x^2}u_{ob} + g.\frac{\partial^3}{\partial x^2 \partial t}u_{ob}\right] - \tau_b \\ &-m_b\frac{\partial^2}{\partial t^2}u_{ot} - \frac{m_c}{6}\frac{\partial^2}{\partial t^2}u_{ot} - \frac{m_c}{3}\frac{\partial^2}{\partial t^2}u_{ob} \\ &+\frac{m_c d_t}{12}\frac{\partial^3}{\partial t^2 \partial x}w_t - \frac{m_c d_b}{6}\frac{\partial^3}{\partial t^2 \partial x}w_b \\ &+m_{1b}\frac{\partial^3}{\partial t^2 \partial x}w_b = 0, \end{aligned} \quad (51)$$

$$\begin{aligned} &-E^t I_t\left[\frac{\partial^4}{\partial x^4}w_t + g.\frac{\partial^5}{\partial x^4 \partial t}w_t\right] + \frac{bd_t}{2}\frac{\partial \tau}{\partial x} \\ &+\left(\frac{E_c b(w_b - w_t)}{c} + \frac{gE_c b}{c}\left[\frac{\partial}{\partial t}w_b - \frac{\partial}{\partial t}w_t\right] + \frac{c}{2}\frac{\partial \tau}{\partial x}\right)b \\ &-m_t\frac{\partial^2}{\partial t^2}w_t - \frac{m_c d_t}{6}\frac{\partial^3}{\partial t^2 \partial x}u_{ot} - \frac{m_c d_b}{12}\frac{\partial^3}{\partial t^2 \partial x}u_{ob} \\ &+\frac{m_c d_t^2}{12}\frac{\partial^3}{\partial t^2 \partial x}w_t - \frac{m_c d_b d_t}{24}\frac{\partial^3}{\partial t^2 \partial x}w_b \\ &-m_{1t}\frac{\partial^3}{\partial t^2 \partial x}u_{ot} + m_{2t}\frac{\partial^4}{\partial t^2 \partial x^2}w_t \\ &-\frac{m_c}{6}\frac{\partial^2}{\partial t^2}w_b - \frac{m_c}{3}\frac{\partial^2}{\partial t^2}w_t = 0, \end{aligned} \quad (52)$$

$$\begin{aligned} &-E^b I_b\left[\frac{\partial^4}{\partial x^4}w_b + g.\frac{\partial^5}{\partial x^4 \partial t}w_b\right] + \frac{bd_b}{2}\frac{\partial \tau}{\partial x} \\ &-\left(\frac{E_c(w_b - w_t)}{c} + \frac{E_c g}{c}\left[\frac{\partial}{\partial t}w_b - \frac{\partial}{\partial t}w_t\right] - \frac{c}{2}\frac{\partial \tau}{\partial x}\right)b \\ &-m_b\frac{\partial^2}{\partial t^2}w_b + \frac{m_c d_b}{12}\frac{\partial^3}{\partial t^2 \partial x}u_{ot} + \frac{m_c d_b}{6}\frac{\partial^3}{\partial t^2 \partial x}u_{ob} \\ &+\frac{m_c d_b^2}{12}\frac{\partial^3}{\partial t^2 \partial x}w_b - \frac{m_c d_b d_t}{24}\frac{\partial^3}{\partial t^2 \partial x}w_t \\ &-m_{1b}\frac{\partial^3}{\partial t^2 \partial x}u_{ob} + m_{2b}\frac{\partial^4}{\partial t^2 \partial x^2}w_b - \frac{m_c}{6}\frac{\partial^2}{\partial t^2}w_t \\ &-\frac{m_c}{3}\frac{\partial^2}{\partial t^2}w_b - +kg_1 cos^2(\theta)\frac{\partial^2}{\partial x^2}w_b \\ &+kg_2 s i n^2(\theta)\frac{\partial^2}{\partial x^2}w_b - k_w w_b - cd = 0, \end{aligned} \quad (53)$$

$$\begin{aligned} &u_{0t}b - u_{0b}b - \frac{b(c - d_t)}{2}\frac{\partial w_t}{\partial x} \\ &-\frac{b(c - d_b)}{2}\frac{\partial w_b}{\partial x} - \frac{bc^3}{12E_c}\frac{\partial^2 \tau}{\partial x^2} - \frac{\tau_b c}{G_c} = 0, \end{aligned} \quad (54)$$

3. Solution method

Base on Navier method, the displacements of the sandwich nano beam with simply supported boundary condition can be written as (Kutlu *et al*. 2012)

$$u_{0t}(x,t) = U_t.cos\left(\frac{n.\pi.x}{l}\right).e^{\omega.t} \quad (55)$$

$$u_{0b}(x,t) = U_b.cos\left(\frac{n.\pi.x}{l}\right).e^{\omega.t} \quad (56)$$

$$w_b(x,t) = W_b.sin\left(\frac{n.\pi.x}{l}\right).e^{\omega.t} \quad (57)$$

$$w_t(x,t) = W_t.sin\left(\frac{n.\pi.x}{l}\right).e^{\omega.t} \tag{58}$$

$$\tau(x,t) = \tau_0.cos\left(\frac{n.\pi.x}{l}\right).e^{\omega.t} \tag{59}$$

where, n is vibration mode number and ω is frequency. Substituting Eqs (55)-(59) into Eqs. (50)-(54), the motion equations in matrix form can be express as

$$\begin{bmatrix} m_{11} & m_{12} & m_{13} & m_{14} & m_{15} \\ m_{21} & m_{22} & m_{23} & m_{24} & m_{25} \\ m_{31} & m_{32} & m_{33} & m_{34} & m_{35} \\ m_{41} & m_{42} & m_{43} & m_{44} & m_{45} \\ m_{51} & m_{52} & m_{53} & m_{54} & m_{55} \end{bmatrix} \ddot{X} + \begin{bmatrix} c_{11} & c_{12} & c_{13} & c_{14} & c_{15} \\ c_{21} & c_{22} & c_{23} & c_{24} & c_{25} \\ c_{31} & c_{32} & c_{33} & c_{34} & c_{35} \\ c_{41} & c_{42} & c_{43} & c_{44} & c_{45} \\ c_{51} & c_{52} & c_{53} & c_{54} & c_{55} \end{bmatrix} \dot{X} + \begin{bmatrix} k_{11} & k_{12} & k_{13} & k_{14} & k_{15} \\ k_{21} & k_{22} & k_{23} & k_{24} & k_{25} \\ k_{31} & k_{32} & k_{33} & k_{34} & k_{35} \\ k_{41} & k_{42} & k_{43} & k_{44} & k_{45} \\ k_{51} & k_{52} & k_{53} & k_{54} & k_{55} \end{bmatrix} X = 0 \tag{6}$$

where $X = \{U_t, U_b, W_t, W_b, T_0\}$ is dynamic vector, $[m_{ij}]$ is mass matrix, $[c_{ij}]$ is damper matrix and $[k_{ij}]$ is matrix stiffness which are expanded in Appendix A.

4. Numerical result and discussion

In this section, a parametric study is done for the effects of different parameters on the linear frequency of the sandwich structure. For this purpose, top and bottom beams have Young's modulus of $E_t = E_b = 210\,GPa$, Poisson's ratio of $\upsilon_m = 0.3$, density of $\rho_t = \rho_b = 2680\,Kg/m^3$, thickness of top and bottom beams is $h = 2\,cm$, the length of beams is $l = 80.4\,cm$ and Width of beams is $b = 5.54\,cm$ which is reinforced by CNTs with Young's modulus of $E_r = 1\,GPa$, Poisson's ratio of $\upsilon_r = 0.3$ and density of $\rho_m = 7800\,Kg/m^3$. The core has Young's modulus of $E_c = 201.74\,MPa$, Poisson's ratio of $\upsilon_m = 0.3$, density of $\rho_c = 32.8\,Kg/m^3$ and Thickness of $h = 1\,cm$.

4.1 Validation

For validating, the structure frequency of this paper without considering viscoelastic parameters, Agglomeration effect and Pasternak orthotropic medium, is compared with Frostig (2003) and Khalili *et al.* (2013).

Considering mechanical properties and geometrical parameter the same as Frostig (2003) and Khalili *et al.* (2013), frequency of sandwich nano beam for five vibration modes is calculated and shown in Table 1.

4.2 Effect of different parameters

Figs. 2 and 3 show the effect of different viscoelastic parameter of medium and damping structure on the frequency versus volume percent of CNTs, respectively .As it is inferred with increasing viscoelastic parameter of medium and damper of structure, the system frequency has reduction**.** It is because with increasing damper of structure, the energy depreciation of the structure will be increased and it can be found that considering with viscoelastic parameter, frequency is decreased. In addition, increasing volume percent of CNTs, frequency is increased. It is because Increase of CNTs leads to higher stiffness.

Table 1 Comparison of frequency of sandwich beam with Frostig (2003) and Khalili *et al.* (2013)

Frequencies (Hz)	Present model	Frostig (2003)	Khalili *et al.* (2013)
Mode 1	250.7717	263	251
Mode 2	534.3375	-	537
Mode 3	866.5572	889	874
Mode 4	1265.4	1289	1282
Mode 5	1742.5	1774	1771

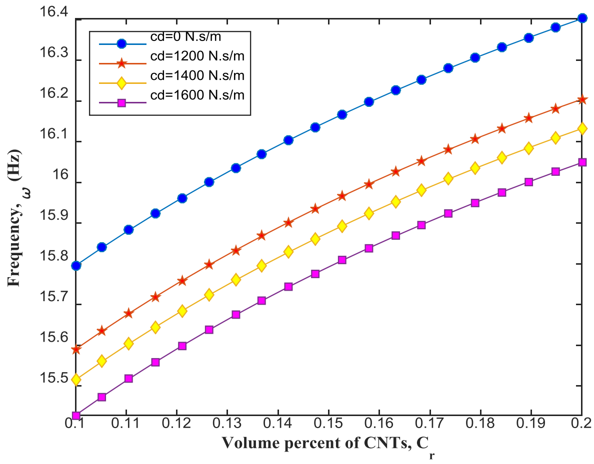

Fig. 2 frequency versus volume percent of CNTs for different damping of structure

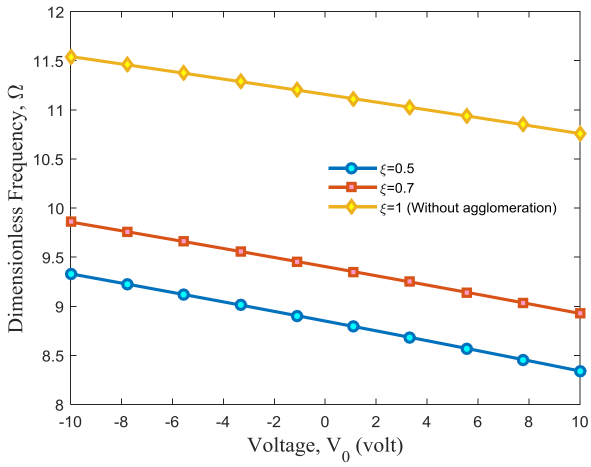

Fig. 3 The effect of viscoelastic parameter on the frequency versus CNTs volume percent

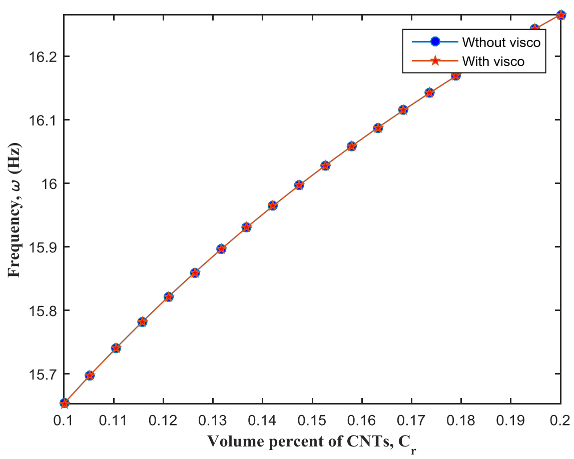

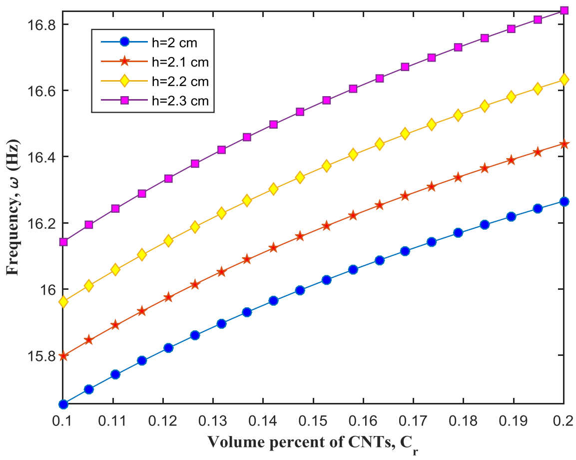

Fig. 4 The effect thickens on the frequency versus CNTs volume percent

Fig. 5 indicates the effect of spring constant of elastic medium on the frequency with respect to CNTs volume percent. It is observed that with increasing spring constant of elastic medium, the frequency is increased. It is because stiffness of system is increased with enhancing spring constant of elastic medium.

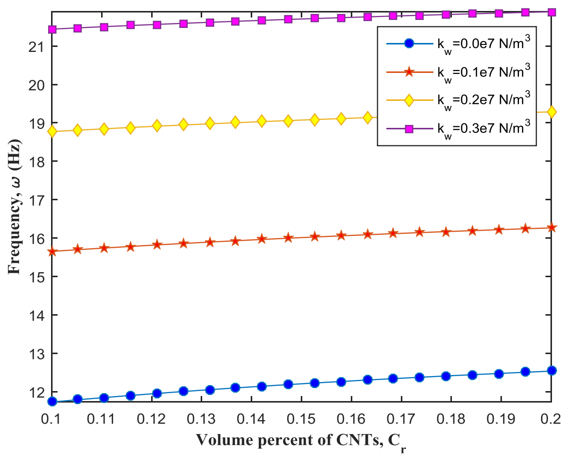

Fig. 5 The effect of spring constant of elastic medium on the frequency versus CNTs volume percent

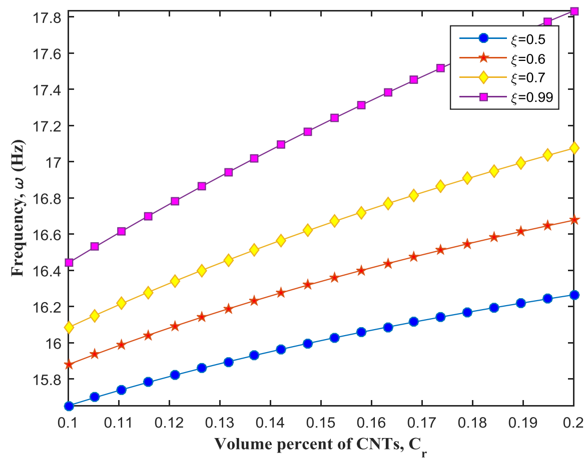

Fig. 6 The effect of agglomeration on the frequency as function of CNTs volume percent

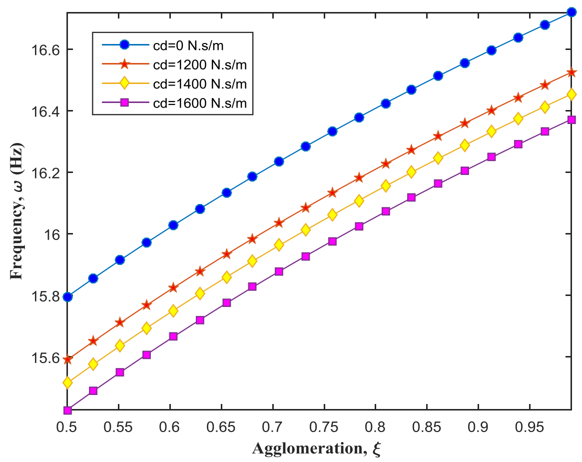

Fig. 7 Frequency versus agglomeration for different damping of elastic medium

The effect of agglomeration on the frequency as function of CNTs volume percent is shown in Fig. 6. With increasing agglomeration effect, frequency decreases. It is because stiffness of structure is decreased.

Fig. 7 shows frequency versus agglomeration for different damping of elastic medium. As can be seen, the frequency of micro sandwich structure with increasing damping of elastic medium is decreased. It is because with increasing damping of elastic medium, the energy depreciation of the structure will be increased. In addition, increasing agglomeration, frequency is decreased. It is because increase of CNTs agglomeration leads to lower stiffness.

The effect of CNTs volume percent on the frequency versus agglomeration is shown in Fig. 8. It is found that with increasing the CNTs volume percent, the frequency is increased due to the enhance in the stiffness of the structure.

Fig. 9 The effect of top and bottom thickens of the structure on the frequency versus CNTs agglomeration. As can be seen, with increasing the thickens, the frequency is increased. It is since with increasing the thickens, the stiffness is increased.

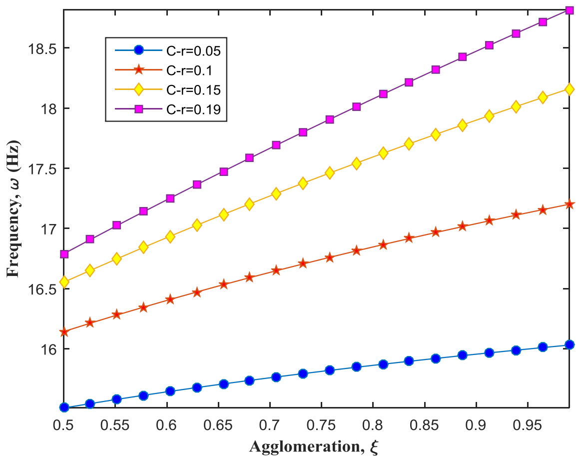

Fig. 8 The effect of CNTs volume percent on the frequency versus agglomeration

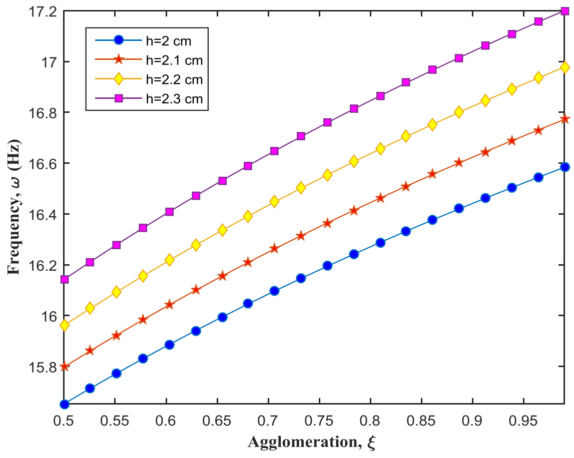

Fig. 9 The effect of thickens on the frequency versus agglomeration

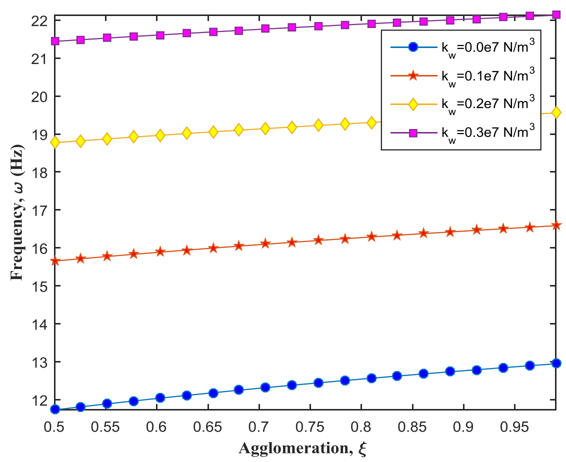

Fig. 10 The effect of spring constant of elastic medium on the frequency versus agglomeration

Fig. 10 indicates the effect of spring constant of elastic medium on the frequency with respect to agglomeration. It is observed that with increasing spring constant of elastic medium, the frequency is increased. It is because stiffness of system is increased with enhancing spring constant of elastic medium.

5. Conclusions

In this work, free vibration of the sandwich structures reinforced with CNTs considering agglomeration effect resting on orthotropic Pasternak was presented. The Mori-Tanaka model for considering effect of agglomeration was used. The size effect applying Eringen's theory was investigated. The Kelvin-voigt model for utilizing structural damping was assumed. The motion equations were calculated by Hamilton's principle and energy method. Using analytical method, the frequency of the structure was obtained. Increasing volume percent of CNTs, frequency was increased. Increasing spring constant of elastic medium, the frequency was increased. With increasing agglomeration effect, frequency decreases. The increasing of CNTs volume percent, frequency was increased.

References

Bennai, R., Ait Atmane, H. and Tounsi, A. (2015), "A new higher-order shear and normal deformation theory for functionally graded sandwich beams", *Steel Compos. Struct., Int. J.*, **19**(3), 521-546. https://doi.org/10.12989/scs.2015.19.3.521

Chan, D.Q., Anh, V.T.T. and Duc, N.D. (2018), "Vibration and nonlinear dynamic response of eccentrically stiffened functionally graded composite truncated conical shells in thermal environments", *Acta Mech*., **230**, 157-178. https://doi.org/10.1007/s00707-018-2282-4

Chung, D.N., Dinh, N.N., Hui, D., Duc, N.D., Trung, T.Q. and Chipara, M. (2013), "Investigation of Polymeric Composite Films Using Modified TiO_2 Nanoparticles for Organic Light Emitting Diodes", *J. Current Nanosci*., **9**, 14-20. https://doi.org/10.2174/157341313805118018

Duc, N.D. (2014a), *Nonlinear Static and Dynamic Stability of Functionally Graded Plates and Shells*, Vietnam National University Press, Hanoi, Vietnam.

Duc, N.D. (2014b), "Nonlinear dynamic response of imperfect eccentrically stiffened FGM double curved shallow shells on elastic foundation", *J. Compos. Struct*., **99**, 88-96. https://doi.org/10.1016/j.compstruct.2012.11.017

Duc, N.D. (2016), "Nonlinear thermal dynamic analysis of eccentrically stiffened S-FGM circular cylindrical shells surrounded on elastic foundations using the Reddy's third-order shear deformation shell theory", *Eur. J. Mech. – A/Solids*, **58**, 10-30. https://doi.org/10.1016/j.euromechsol.2016.01.004

Duc, N.D. and Minh, D.K. (2010), "Bending analysis of three-phase polymer composite plates reinforced by glass fibers and Titanium oxide particles", *J. Computat. Mat. Sci*., **49**, 194-198. https://doi.org/10.1016/j.commatsci.2010.04.016

Duc, N.D., Quan, T.Q. and Nam, D. (2013), "Nonlinear stability analysis of imperfect three phase polymer composite plates", *J. Mech. Compos. Mater*., **49**, 345-358. https://doi.org/10.1007/s11029-013-9352-4

Duc, N.D., Hadavinia, H., Thu, P.V. and Quan, T.Q. (2015), "Vibration and nonlinear dynamic response of imperfect three-phase polymer nanocomposite panel resting on elastic foundations under hydrodynamic loads", *Compos. Struct*., **131**, 229-237. https://doi.org/10.1016/j.compstruct.2015.05.009

Duc, N.D., Khoa, N.D. and Thiem, H.T. (2018), "Nonlinear thermo-mechanical response of eccentrically stiffened Sigmoid FGM circular cylindrical shells subjected to compressive and uniform radial loads using the Reddy's third-order shear deformation shell theory", *Mech. Adv. Mater. Struct.*, **25**, 1157-1167. https://doi.org/10.1080/15376494.2017.1341581

Dutta, G., Panda. S.K., Mahapatra, T.R. and Singh, V.K. (2017), "Electro-magneto-elastic response of laminated composite plate: A finite element approach", *Int. J. Appl. Computat. Math.*, **3**, 2573-2592. https://doi.org/10.1007/s40819-016-0256-6

Daya, E.M., Azrar, L. and Potier-Ferry, M. (2004), "An amplitude equation for the non-linear vibration of viscoelastically damped sandwich beams", *J. Sound Vib.*, **271**, 789-813. https://doi.org/10.1016/S0022-460X(03)00754-5

Eltaher, M.A., El-Borgi, S. and Reddy, J.N. (2016), "Nonlinear analysis of size-dependent and material-dependent nonlocal CNTs", *Compos. Struct.*, **153**, 902-913. https://doi.org/10.1016/j.compstruct.2016.07.013

Frostig, Y. (2003), "An efficient higher order zigzag theory for composite and sandwich beams subjected to thermal loading", *Int. J. Solids Struct.*, **40**, 6613-6631. https://doi.org/10.1016/j.ijsolstr.2003.08.014

García-Macíasa, E. and Castro-Triguero, R. (2018), "Coupled effect of CNT waviness and agglomeration: A case study of vibrational analysis of CNT/polymer skew plates", *Compos. Struct.*, **193**, 87-102. https://doi.org/10.1016/j.compstruct.2018.03.001

Kapuria, S., Ahmed, A. and Dumir, P.C. (2005), "An efficient coupled zigzag theory for dynamic analysis of piezoelectric composite and sandwich beams with damping", *J. Sound Vib.*, **279**, 345-371. https://doi.org/10.1016/j.jsv.2003.11.018

Khalili, S.M.R., Botshekanan Dehkordi, M., Carrera, E. and Shariyat, M. (2013), "Non-linear dynamic analysis of a sandwich beam with pseudoelastic SMA hybrid composite faces based on higher order finite element theory", *Compos. Struct.*, **96**, 243-255. https://doi.org/10.1016/j.compstruct.2012.08.020

Kolahchi, R. (2017), "A comparative study on the bending, vibration and buckling of viscoelastic sandwich nano-plates based on different nonlocal theories using DC, HDQ and DQ methods", *Aerosp. Sci. Technol.*, **66**, 235-248. https://doi.org/10.1016/j.ast.2017.03.016

Kutlu, A., Uğurlu, B., Omurtag, M.H. and Ergin, A. (2012), "Dynamic response of Mindlin plates resting on arbitrarily orthotropic Pasternak foundation and partially in contact with fluid", *Ocean Eng.*, **42**, 112-125. https://doi.org/10.1016/j.oceaneng.2012.01.010

Lakreb, N., Bezzazi, B. and Pereira, H. (2015), "Mechanical behavior of multilayered sandwich panels of wood veneer and a core of cork agglomerates", *Mater. Des.*, **65**, 627-636.

Li, Z., Chu, J., Yang, C., Hao, S., Bissett, M.A., Kinloch, I.A. and Young, R.J. (2018), "Effect of functional groups on the agglomeration of graphene in Nano composites", *Compos. Sci. Technol.*, **163**, 116-122. https://doi.org/10.1016/j.compscitech.2018.05.016

Lim, J.Y. and Bart-Smith, H. (2015), "An analytical model for the face wrinkling failure prediction of metallic corrugated core sandwich columns in dynamic compression", *Int. J. Mech. Sci.*, **92**, 290-303. https://doi.org/10.1016/j.ijmecsci.2015.01.002

Liu, Y., Yu, K., Hu, H., Belouettar, S., Potier-Ferry, M. and Damil, N. (2012), "A new Fourier-related double scale analysis for instability phenomena in sandwich structures", *Int. J. Solids Struct.*, **49**, 3077-3088. https://doi.org/10.1080/15376494.2015.1085606

Loghman, A. and Cheraghbak, A. (2016), "Agglomeration Effects on Electro-magnetothermo Elastic Behavior of Nano-composite Piezoelectric Cylinder", *Polym. Compos.*, **39**(5), 1594-1603. https://doi.org/10.1002/pc.24104

Madani, H., Hosseini, H. and Shokravi, M. (2016), "Differential cubature method for vibration analysis of embedded FG-CNT-reinforced piezoelectric cylindrical shells subjected to uniform and non-uniform temperature distributions", *Steel Compos. Struct., Int. J.*, **22**(4), 889-913. https://doi.org/10.12989/scs.2016.22.4.889

Mahapatra, T.R. and Panda, S.K. (2016), "Nonlinear free vibration analysis of laminated composite spherical shell panel under elevated hygrothermal environment: A micromechanical approach", *Aerosp. Sci. Technol.*, **49**, 276-288. https://doi.org/10.1016/j.ast.2015.12.018

Mahapatra, T.R., Panda, S.K. and Kar, V.R. (2016a), "Nonlinear flexural analysis of laminated composite panel under hygro-thermo-mechanical loading—A micromechanical approach", *Int. J. Computat. Meth.*, **13**, 1650015. https://doi.org/10.1142/S0219876216500158

Mahapatra, T.R., Panda, S.K. and Kar, V.R. (2016b), "Nonlinear hygro-thermo-elastic vibration analysis of doubly curved composite shell panel using finite element micromechanical model", *Mech. Advan. Mater. Struct.*, **23**, 1343-1359. https://doi.org/10.1080/15376494.2015.1085606

Mahapatra, T.R., Panda, S.K. and Kar, V.R. (2016c), "Geometrically nonlinear flexural analysis of hygro-thermo-elastic laminated composite doubly curved shell panel", *Int. J. Mech. Mat. Des.*, **12**, 153-171. https://doi.org/10.1007/s10999-015-9299-9

Mahi, A., Bedia, E.A.A. and Tounsi, A. (2015), "A new hyperbolic shear deformation theory for bending and free vibration analysis of isotropic, functionally graded, sandwich and laminated composite plates", *Appl. Math. Model.*, **39**, 2489-2508. https://doi.org/10.1016/j.apm.2014.10.045

Mehar, K., Panda, S.K. and Mahapatra, T.R. (2017), "Thermoelastic nonlinear frequency analysis of CNT reinforced functionally graded sandwich structure", *Eur. J. Mech. A/Solids* **65**, 384-396. https://doi.org/10.1016/j.euromechsol.2017.05.005

Mori, T. and Tanaka, K. (1973), "Average stress in matrix and average elastic energy of materials with misfitting inclusions", *Acta Metall. Mater.*, **21**, 571-574. https://doi.org/10.1016/0001-6160(73)90064-3

Nejati, M., Asanjarani, A., Dimitri, R. and Tornabene, F. (2017), "Static and free vibration analysis of functionally graded conical shells reinforced by carbon nanotubes", *Int. J. Mech. Sci.*, **130**, 383-398. https://doi.org/10.1016/j.ijmecsci.2017.06.024

Qin, Q.H. and Wang, T.J. (2009), "A theoretical analysis of the dynamic response of metallic sandwich Beam under impulsive loading", *Eur. J. Mech. A/Solids*, **28**, 1014-1025. https://doi.org/10.1016/j.euromechsol.2009.04.002

Quan, T.Q., Tran, P., Tuan, N.D. and Duc, N.D. (2015), "Nonlinear dynamic analysis and vibration of shear deformable eccentrically stiffened S-FGM cylindrical panels with metal-ceramic-metal layers resting on elastic foundations", *Compos. Struct.*, **126**, 16-33. https://doi.org/10.1016/j.compstruct.2015.02.056

Safaeia, B., Moradi-Dastjerdib, R. and Chu, F. (2018), "Effect of thermal gradient load on thermo-elastic vibrational behavior of sandwich plates reinforced by carbon nanotube agglomerations", *Compos. Struct.*, **192**, 28-37. https://doi.org/10.1016/j.compstruct.2018.02.022

Shokravi, M. (2018), "Forced vibration response in nanocomposite cylindrical shells - Based on strain gradient beam theory", *Steel Compos. Struct., Int. J.*, **28**(3), 381-388. https://doi.org/10.12989/scs.2018.28.3.381

Smyczynski, M.J. and Magnucka-Blandzi, E. (2018), "Stability of five layer sandwich beams – a nonlinear hypothesis", *Steel Compos. Struct., Int. J.*, **28**(6), 671-679. https://doi.org/10.12989/scs.2018.28.6.671

Sorokin, S.V. and Grishina, S.V. (2004), "Analysis of wave propagation in sandwich beams with parametric stiffness modulations", *J. Sound Vib.*, **271**, 1063-1082. https://doi.org/10.1016/j.jsv.2003.03.005

Suman, S.D., Hirwani, C.K., Chaturvedi, A. and Panda, S.K. (2017), "Effect of magnetostrictive material layer on the stress and deformation behaviour of laminated structure", *IOP Conference Series*: *Materials Science and Engineering*, **178**(1), 012026.

Thu, P.V. and Duc, N.D. (2016), "Nonlinear dynamic response and vibration of an imperfect three-phase laminated nanocomposite cylindrical panel resting on elastic foundations in thermal environments", *J. Sci. Eng. Compos. Mater.*, **24**(6), 951-962. https://doi.org/10.1515/secm-2015-0467

Vuong, P.M. and Duc, N.D. (2018), "Nonlinear response and buckling analysis of eccentrically stiffened FGM toroidal shell segments in thermal environment", *Aerosp. Sci. Technol.*, **79**, 383-398. https://doi.org/10.1016/j.ast.2018.05.058

Zeinedini, A., Shokrieh, M.M. and Ebrahimi, A. (2018), "The effect of agglomeration on the fracture toughness of CNTs-reinforced Nano composites", *Theoret. Appl. Fract. Mech.*, **94**, 84-94. https://doi.org/10.1016/j.tafmec.2018.01.009

CC

Appendix A

$$M11 = -mt.lne^2 - (1/3).mc.lne^2 \quad (A1)$$

$$M12 = -(1/6).mc.lne^2 \quad (A2)$$

$$M13 = (1/6).mc.dt.n.Pi.1^2/L + m1t.n.Pi.1^2/L \quad (A3)$$

$$M14 = -(1/12).mc.db.n.Pi.lne^2/L \quad (A4)$$

M15=0 (A5)

$$M21 = -(1/6).mc.lne^2 \quad (A6)$$

$$M22 = -mb.lne^2 - (1/3).mc.lne^2 \quad (A7)$$

$$M23 = (1/12).mc.dt.n.Pi.lne^2/L \quad (A8)$$

$$M24 = -(1/6).mc.db.n.Pi.1^2/L + m1b.n.Pi.1^2/L \quad (A9)$$

M25=0 (A10)

$$M31 = (1/6).mc.dt.n.Pi.1^2/L + m1t.n.Pi.1^2/L \quad (A11)$$

$$M32 = (1/12).mc.db.n.Pi.lne^2/L \quad (A12)$$

$$M33 = -mt - (1/12).mc.dt^2.n^2.Pi^2.1^2/L^2 - m2t.n^2.Pi^2.1^2/L^2; \quad (A13)$$

$$M34=(1/24).mc.db.dt.n^2.Pi^2.1^2/L^2 - (1/6).mc.1^2 \quad (A14)$$

M35=0 (A15)

$$M41 = -(1/12).mc.db.n.Pi.lne^2/L \quad (A16)$$

$$M42 = -(1/6).mc.db.n.Pi.lne^2/L + m1b.n.Pi.1^2/L \quad (A17)$$

$$M43=(1/24).mc.db.dt.n^2.Pi^2.1^2/L^2 - (1/6).mc.1^2 \quad (A18)$$

$$M44 = -mb.lne^2 - (1/12).mc.db^2.n^2.Pi^2.1^2/L^2 - m2b.n^2.Pi^2.1^2/L^2 - (1/3).mc.1^2 \quad (A19)$$

M45=0 (A20)

M51=0 (A21)

M52=0 (A22)

M53=0 (A23)

M54=0 (A24)

M55=0 (A25)

$$C11 = At.E.(-g.n^2.Pi^2.lne/L^2) \quad (A26)$$

C12=0 (A27)

C13=0 (A28)

C14=0 (A29)

C15=0 (A30)

C21=0 (A31)

$$C22 = -(g.n^2.Pi^2.lne/L^2).E.Ab \quad (A32)$$

C23=0 (A33)

C24=0 (A34)

C25=0 (A35)

C31=0 (A36)

C32=0 (A37)

$$C33 = -E.(+g.n^4.Pi^4.lne/L^4).It + (Ec.(-g.lne).b)/(c) \quad (A38)$$

$$C34 = Ec.(g.lne).b/c \quad (A39)$$

C35=0 (A40)

C41=0 (A41)

C42=0 (A42)

$$C43 = -Ec.(-g.lne).b/c \quad (A43)$$

$$C44 = -E.(+g.n^4.Pi^4.lne/L^4).Ib - Ec.(g.lne).b/c - cd \quad (A44)$$

C45=0 (A45)

C51=0 (A46)

C52=0 (A47)

C53=0 (A48)

C54=0 (A49)

C55=0 (A50)

$$K11 = -n^2.Pi^2/L^2.At.E \quad (A51)$$

K12=0 (A52)

K13=0 (A53)

K14=0 (A54)

K15=b (A55)

K21=0 (A56)

$$K22 = -n^2.Pi^2/L^2.E.Ab \tag{A57}$$

K23=0 (A58)

K24=0 (A59)

K25=-b (A60)

K31=0 (A61)

K32=0 (A62)

$$K33 = -E.(n^4.Pi^4/L^4).It + (Ec.(-1).b)/(c) \tag{A63}$$

$$K34 = Ec.(+1).b/c \tag{A64}$$

K35=-(1/2).n.Pi.b.dt/L-(1/2).C.n.Pi.b/L (A65)

K41=0 (A66)

K42=0 (A67)

$$K43 = -Ec.(-1).b/c \tag{A68}$$

$$\begin{aligned} &K44 = -E.(n^4.Pi^4/L^4).Ib - Ec.(+1).b/c - \\ &kg1.cos(theta)^2.n^2.Pi^2/L^2 \\ &\qquad - kg2.sin(theta)^2.n^2.Pi^2/L^2 \\ &\qquad - Kw \end{aligned} \tag{A69}$$

K45=-(1/2).n.Pi.b.db/L-(1/2).C.n.Pi.b/L (A70)

K51=b (A71)

K52=-b (A72)

$$\begin{aligned} &K53 = -(1/2).n.Pi.b.(c+dt)/L \\ &-(1/2).k.n^3.Pi^3.b.(c+dt)/L^3 \end{aligned} \tag{A73}$$

$$K54 = -(1/2).n.Pi.b.(c+db)/L \tag{A74}$$

$$\begin{aligned} &K55 = (1/12).n^2.Pi^2.b.c^3/(L^2.Ec) \\ &+b.c/Gc \end{aligned} \tag{A75}$$